Theoretical Study on Gas-phase Pyrolytic Reactions of *N*-Ethyl, *N*-Isopropyl and *N*-*t*-Butyl Substituted 2-Aminopyrazine

CHEN, Li-Ping(陈丽萍) **HONG, San-Guo***(洪三国)
Department of Chemistry, Jiangxi Normal University, Nanchang, Jiangxi 330027, China

Density functional theory (DFT) and *ab initio* methods were used to study gas-phase pyrolytic reaction mechanisms of *N*-ethyl, *N*-isopropyl and *N*-*t*-butyl substituted 2-aminopyrazine at B3LYP/6-31G* and MP2/6-31G*, respectively. Single-point energies of all optimized molecular geometries were calculated at B3LYP/6-311 + G(2d,p) level. Results show that the pyrolytic reactions were carried out through a unimolecular first-order mechanism which were caused by the migration of atom H(17) via a six-member ring transition state. The activation energies which were verified by vibrational analysis and correlated with zero-point energies along the reaction channel at B3LYP/6-311 + G(2d,p) level were 252.02 kJ·mol^{-1}(*N*-ethyl substituted), 235.92 kJ·mol^{-1}(*N*-isopropyl substituted) and 234.27 kJ·mol^{-1}(*N*-*t*-butyl substituted), respectively. The results were in good agreement with available experimental data.

Keywords 2-aminopyrazine, pyrolytic reaction, density functional theory, *ab initio*, transition state

Introduction

Aminopyrazine can be used as inhibitor for assembly of protease[1] and as antagonist[2] for glutamate. Research results show that aminopyrazine plays an effective role in pharmaceutical synthesis of anti-cancer and anti-HIV virus drugs.[2,3] Recently, much attention was paid to its properties and applications due to its importance in chemistry and biochemistry. Experimental results[4-7] showed that the gas-phase pyrolytic reactions of 2-alkoxypyrimidines and 2-alkoxypyrazines were carried out through a unimolecular first-order thermal elimination process with products of alkenes and 2(1*H*)-pyrimidinone/2(1*H*)-pyrazinone via a six-member ring transition state. Further experimental results of Al-Awadi *et al.*[8] showed that the pyrolytic reactions of 2-*N*-alkylamino and 2-alkoxypyrazines actually involved the same six-member ring transition state (Scheme 1) when oxygen atoms of the alkoxy heterocycles were replaced by amino analogues.

But till now, no theoretical studies on this type of pyrolytic reaction have been seen. In order to provide detailed insights into the nature of this type of reaction and provide useful information to experimental researchers, based on our former studies on this reaction system (semi-empirical PM3 methods and *ab initio* calculations at RHF/6-31G level),[9] recently, we performed a further study on the gas-phase pyrolytic reaction mechanisms of *N*-ethyl, *N*-isopropyl and *N*-*t*-butyl substituted 2-aminopyrazine at level of MP2/6-31G*[10] and B3LYP/6-31G*,[11,12] respectively.

Computational methods

All calculations were performed with *Gaussian 98*[13] program package. The geometries of reactants (Re), transition states (TS) and products (P) were optimized by Berny method[14] at MP2/6-31G*[15] level, except for *N*-*t*-butyl substituted 2-aminopyrazine which can not achieve convergence at MP2/6-31G* level and thus was optimized at B3LYP/6-31G* level. The transition state structures were identified by vibrational analysis, whose fully optimized structures are first-order saddle points characterized by only one imaginary frequency. For a more accurate evaluation of energies along the reaction channel, single point calculation at higher level of B3LYP/6-311 + G(2d,p)[16,17] were performed on above optimized geometries. And last, the reaction pathway of *N*-ethyl substituted 2-aminopyrazine was traced forward and backward by intrinsic reaction coordinate (IRC)[18] method.

Results and discussion

Outline of the reaction channel and the atomic numbering are shown in Scheme 1.

N-Ethyl substituted 2-aminopyrazine

The optimized geometric parameters of *N*-ethyl substituted 2-aminopyrazine (Re) and its pyrolytic reaction product (P) calculated at MP2/6-31G* level are listed in Table 1, the geometric parameters of transition state (TS) are also listed in Table 1. The energies calculated at B3LYP/6-311 + G(2d,p) level along the reaction channel for *N*-ethyl (**1**), *N*-isopropyl (**2**) and *N*-*t*-butyl (**3**) substituted 2-aminopyrazine are shown in Table 2.

* E-mail: hsg@ncu.edu.cn; clpchen@hotmail.com
Received April 23, 2002; revised August 8, 2002; accepted September 24, 2002.

Scheme 1 The reaction mechanism of the gas-phase pyrolytic reactions of *N*-ethyl (**1**), *N*-isopropyl (**2**) and *N*-*t*-butyl (**3**) substituted 2-aminopyrazine

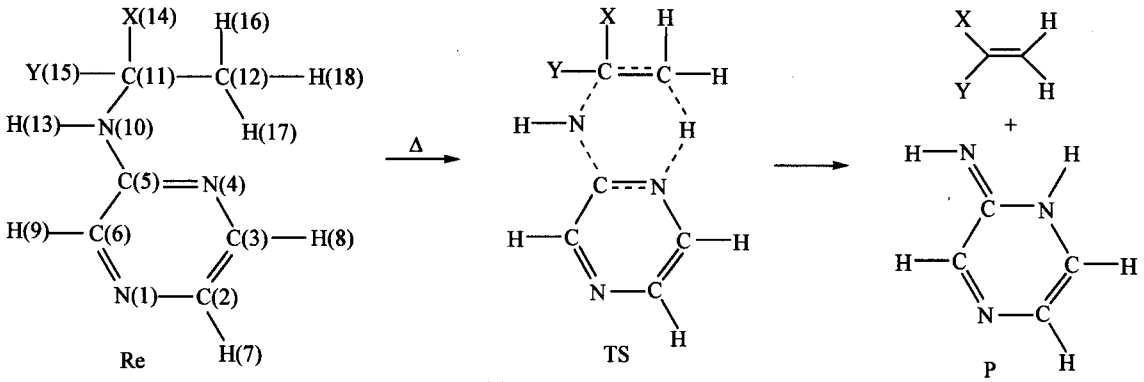

(**1**) X = H, Y = H; (**2**) X = CH_3, Y = H; (**3**) X = CH_3, Y = CH_3

Table 1 Geometric parameters of Re, TS and P (bond lengths are in nm, bond angles and dihedral angles are in degree)

Parameter	Re	TS	P	Parameter	Re	TS	P
R(2-1)	0.13514	0.13689	0.13794	∠3-2-1	121.5559	122.3773	121.4154
R(3-2)	0.13884	0.13719	0.13645	∠4-3-2	122.7525	120.6818	119.7327
R(4-3)	0.13478	0.13667	0.13631	∠5-4-3	116.0299	118.8981	123.3836
R(5-4)	0.13456	0.13789	0.13927	∠6-5-4	120.9393	114.8283	112.0130
R(6-5)	0.14155	0.14337	0.14626	∠10-5-4	118.2066	114.7642	118.6339
R(10-5)	0.13768	0.13332	0.12979	∠10-5-6	120.8541	126.2572	129.3531
R(11-10)	0.14590	0.19989	0.33662	∠16-12-11	110.5932	118.2155	121.7073
R(12-11)	0.15257	0.13980	0.13401	∠17-12-11	110.8480		
R(13-10)	0.10141	0.10264	0.10238	∠17-4-5		105.6734	115.7356
R(17-12)	0.10944	0.15083	0.25918	∠17-12-11-10	59.4690		
R(17-4)	0.27320	0.11836	0.10211	∠17-4-3-2		138.0614	
				∠17-4-5-10			-0.1102

Table 2 Total energies E_t, zero-point energies of Re, TS and P, energy differences ΔE, activation energies E_a

Parameter	E_t(Hartree)	ZPE (kJ·mol^{-1})	ΔE (kJ·mol^{-1})	E_a(kJ·mol^{-1})	E_a(exp.)(kJ·mol^{-1})
Re (1)	-398.4242848	425.7563			
TS (1)	-398.3232101	412.4057	113.36	252.02	235.68 ± 0.78
P (1)	-398.3776343	416.6380			
Re (2)	-437.7478869	505.0070			
TS (2)	-437.6524328	490.3121	92.36	235.92	218.20 ± 0.14
P (2)	-437.7096089	496.8680			
Re (3)	-477.0745424	582.8636			
TS (3)	-476.9796663	568.0374	82.32	234.27	202.62 ± 0.15
P (3)	-477.0409073	576.8801			

According to Scheme 1 and data listed in Table 1, we can see that, for pyrolytic reaction process of *N*-ethyl 2-aminopyrazine, from reactant (Re) to product (P) via transition state (TS), the distance between atoms N(4)—H(17) is gradually shortened, from Re's far away via TS's 0.11836 nm to P's 0.10211 nm, at P state, a single bond has been formed between atoms N(4)—H(17). While the distances between N(10)—C(11) and C(12)—H(17) are gradually prolonged, from Re's 0.1459 nm and 0.10944 nm via TS's 0.19989 nm and 0.15083 nm to P's 0.33662 nm and 0.25918 nm, respectively, at P state, bonds N(10)—C(11) and C(12)—H(17) are actually broken. At transition state (TS), atoms N(4), C(5), N(10), C(11), C(12) and H(17) seem to form a six-member ring. It should be reasonably concluded that *N*-ethyl substituted 2-aminopyrazine undergoes unimolecular first-order pyrolytic reaction via a six-member ring transition state.

Vibration analysis of the transition state (TS) showed that Hessian matrix has only one negative eigenvalue. The displacement vectors associated with mode of imaginary vibration (Fig. 1) clearly connect reactant (Re) and product (P). This confirms that the transition state (TS) optimized by Berny method is reliable. The reaction pathway of this pyrolysis was traced using IRC theory (shown in Fig. 2).

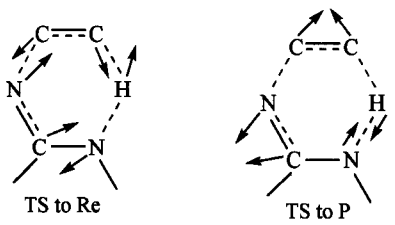

Fig. 1 Modes of the imaginary vibration of TS.

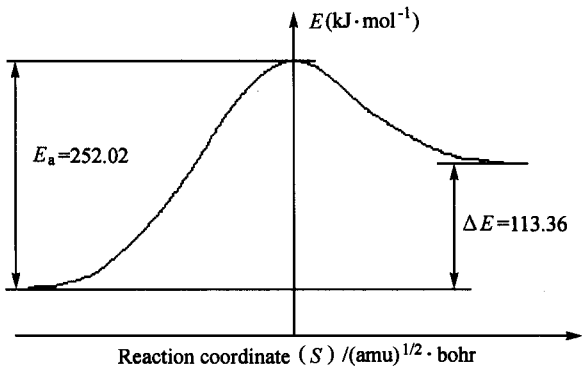

Fig. 2 The potential energy profile of the IRC pathway.

Starting from TS and stepping down along direction towards reactant (Re) and product (P), the potential energy profile of intrinsic reaction coordinate (IRC) pathway was obtained. Correlated by zero-point energy (ZPE) $E_v = 0$, the energy difference $\Delta E = (E_P - E_{Re})$ of the reaction is 113.36 kJ·mol^{-1}, the activation energy $E_a = (E_{TS} - E_{Re})$ is 252.02 kJ·mol^{-1}. The reaction is an endothermic one. Compared the structure (Table 1) and energy (Table 2) of the transition state (TS) with those of reactant (Re) and product (P), the transition state (TS) is much close to product (P), this is in consistent with the Bell-Evans-Polanyi (BEP) principle,[19] which says an endothermic reaction leads to a later TS state, and vice versa, an exothermic reaction leads to an early TS state.

The net charges of atom H(17) and N(4) along IRC pathway are shown in Table 3, bond distances between N(4)—H(17) along the IRC pathway are also shown in Table 3. It can be seen that from $S = -8.0$ to $S = 8.0$ (from Re to P), the net charges of atom H(17) increase gradually from Re's 0.1941 to TS's 0.5045, then decrease gradually to P's 0.4054, while the net charge changes of N(4) were vice versa, from Re's −0.7413 gradually decrease to TS's −1.0131, then gradually increase to P's −0.9794. While the bond distances between N(4)—H(17) are gradually shortened from $S = -8.0$ to $S = 8.0$ till a single bond is formed. This means that during the pyrolytic reaction process of *N*-ethyl substituted 2-aminopyrazine, as H(17) gradually approaches N(4), the bond distance between N(4)—H(17) is gradually shortened, some electrons migrate from N(4) to H(17), which leads to the formation of a single bond between N(4)—H(17).

N-Isopropyl and N-t-butyl substituted 2-aminopyrazine

Calculations show that the mechanism of gas-phase pyrolytic reactions of *N*-isopropyl, and *N*-*t*-butyl substituted 2-aminopyrazine is similar to that of *N*-ethyl substituted 2-aminopyrazine (Scheme 1). The optimized geometric parameters for *N*-isopropyl and *N*-*t*-butyl substituted 2-aminopyrazine are listed in Table 4, the energy differences ΔE ($E_P - E_{Re}$) and activation energies E_a ($E_{TS} - E_{Re}$) are shown in above Table 2. It can be seen from Table 2 that the energy difference of *N*-*t*-butyl substituted 2-aminopyrazine is lower than that of *N*-isopropyl substituted 2-aminopyrazine, and both are lower than that of *N*-ethyl substituted 2-aminopyrazine. Considering the electronic and space effects, we can conclude that methyl make the transition states more stable than that of ethyl.

From data listed in Table 2, it is clear that the order of reaction activation energy E_a for the three compounds is the same as the order of energy differences ΔE: *N*-ethyl > *N*-isopropyl > *N*-*t*-butyl. Correlated by the zero-point energy (ZPE), the calculated activation energy at high level of B3LYP/6-311 + G(2d, p) (Table 2) are in good agreement with available experimental data.

Conclusions

The mechanisms of gas-phase pyrolytic reactions of *N*-ethyl, *N*-isopropyl and *N*-*t*-butyl substituted 2-aminopyrazine were investigated at MP2/6-31G* and B3LYP/6-31G* level, a valid reaction channel was established.

(1) *N*-ethyl, *N*-isopropyl and *N*-*t*-butyl substituted 2-aminopyrazine undergo unimolecular first-order pyrolytic reactions via a six-member ring transition state, the migration of atom H(17) caused the reaction. (2) The reactions are endothermic with energy difference 113.36 kJ·mol^{-1}, 92.36 kJ·mol^{-1}, and 82.32 kJ·mol^{-1}, respectively, the activation energy is 252.02 kJ·mol^{-1}, 235.92 kJ·mol^{-1} and 234.27 kJ·mol^{-1}, respectively. (3) Due to space and electron effects of different substituents, the order of reaction activation is: *N*-ethyl > *N*-isopropyl > *N*-*t*-butyl.

The results would be helpful for further experimental and theoretical study of this reaction.

Table 3 The charge and distance between atom N(4), H(17) along the IRC pathway

S	−8.0	−6.0	−4.0	−2.0	0	2.0	4.0	6.0	8.0
N(4)	−0.7413	−0.7554	−0.8085	−0.8697	−1.0131	−0.9983	−0.9873	−0.9811	−0.9794
H(17)	0.1941	0.2274	0.2678	0.3251	0.5045	0.4613	0.4386	0.4123	0.4054
R(4-17)	0.2732	0.2321	0.1851	0.1387	0.1184	0.1098	0.1063	0.1038	0.1021

Table 4 Geometric parameters of Re, TS and P (bond lengths are in nm, bond angles and dihedral angles are in degree)

Parameter	Re		TS		P	
	N-Isopropyl	*N*-*t*-Butyl	*N*-Isopropyl	*N*-*t*-Butyl	*N*-Isopropyl	*N*-*t*-Butyl
R(2-1)	0.13517	0.13482	0.13691	0.13659	0.13789	0.13785
R(3-2)	0.13876	0.13870	0.13720	0.13732	0.13647	0.13618
R(4-3)	0.13483	0.13407	0.13664	0.13552	0.13630	0.13624
R(5-4)	0.13468	0.13401	0.13789	0.13755	0.13914	0.13958
R(6-5)	0.14179	0.14280	0.13208	0.13087	0.14620	0.14686
R(10-5)	0.13736	0.13695	0.13320	0.13242	0.12987	0.12910
R(11-10)	0.14693	0.14822	0.20357	0.21812	0.37369	0.36738
R(12-11)	0.15289	0.15345	0.13983	0.14113	0.13429	0.13424
R(13-10)	0.10133	0.10120	0.10269	0.10222	0.10237	0.10214
R(17-12)	0.10911	0.10965	0.14907	0.14162	0.24574	0.24571
R(17-4)	0.25169	0.26192	0.11924	0.12619	0.10222	0.10210
∠3-2-1	121.4686	120.6663	122.3405	121.3393	121.3800	121.0965
∠4-3-2	122.8744	123.1684	120.7430	121.4269	119.7833	120.0843
∠5-4-3	116.1173	116.6701	118.8817	119.1385	123.3365	122.9164
∠6-5-4	120.6039	119.8823			112.0589	112.1419
∠10-5-4	119.4286	121.9350	114.7491	116.0185	118.8311	119.2470
∠10-5-6	119.9676	118.1832			129.1099	128.6111
∠16-12-11	110.0482	107.8621	117.7271	117.4882	121.3554	121.6359
∠17-12-11	110.2036	111.9394				
∠17-4-5			105.1221	104.8692	116.6470	116.9260
∠17-12-11-10	65.4321	60.5051				
∠17-4-5-10					0.547	−0.043

References

1 Hellberg, M.; Stubbins, J. F.; Glennon, R. A. *Bioorg. Med. Chem.* **2000**, *8*, 1917.

2 Ikomomidon, H. *EP 1 002 535*, **2000** [*Chem. Abstr.* **2000**, *133*, 790].

3 Besterman, J. M. *US 6 100 273*, **2000** [*Chem. Abstr.* **2000**, *133*, 150767].

4 Taylor, R. *J. Chem. Soc., Chem. Commun.* **1978**, (16), 722.

5 Al-Awadi, N. A.; Ballam, J.; Hamblade, P. R.; Taylor, R. *J. Chem. Soc., Perkin Trans. 2* **1982**, (9), 1175.

6 Al-Awadi, N. A.; Taylor, R. *J. Chem. Soc., Perkin Trans. 2* **1986**, (2), 1255.

7 Al-Awadi, N. A.; Taylor, R. *J. Chem. Soc., Perkin Trans. 2* **1986**, (2), 1585.

8 Al-Awadi, N. A.; El-Dusouqui, O. M. E. *Int. J. Chem. Kinet.* **2000**, *32*, 403.

9 Chen, L.-P.; Hong, S.-G. *Jiangxi Shifan Daxue Xuebao* **2002**, *26*, 105 (in Chinese).

10 Frisch, M. J.; Head-Gordon, M.; Pople, J. A. *Chem. Phys. Lett.* **1990**, *166*, 281.

11 Becke, A. D. *J. Chem. Phys.* **1993**, *98*, 5648.

12 Lee, C.; Yand, W.; Parr, R. G. *Phys. Rev. B* **1998**, *37*, 785.

13 Frisch, M. J.; Trucks, G. W.; Schlegel, H. B.; Scuseria, G. E.; Robb, M. A.; Cheeseman, J. R.; Zakrzewski, V. G.; Montgomery, J. A.; Stratmann, Jr. R. E.; Burant, J. C.; Dapprich, S.; Millam, J. M.; Daniels, A. D.; Kudin, K. N.; Strain, M. C.; Farkas, O.; Tomasi, J.; Barone, V.; Cossi, M.; Cammi, R.; Mennucci, B.; Pomelli, C.; Adamo, C.; Clifford, S.; Ochterski, J.; Petersson, G. A.; Ayala, P. Y.; Cui, Q.; Morokuma, K.; Malick, D. K.; Rabuck, A. D.; Raghavachari, K.; Foresman, J. B.; Cioslowski, J.; Ortiz, J. V.; Baboul, A. G.; Stefanov, B. B.; Liu, G.; Liashenko, A.; Piskorz, P.; Komaromi, I.; Gomperts, R.; Martin, R. L.; Fox, D. J.; Keith, T.; Al-Laham, M. A.; Peng, C. Y.; Nanayakkara, A.; Gonzalez, C.; Challacombe, M.; Gill, P. M. W.; Johnson, B.; Chen, W.; Wong, M. W.; Andres, J. L.; Head-Gordon, M.; Replogle, E. S.; Pople, J. A. *Gaussian 98*, Revision A. 7, Gaussian, Inc., Pittsburgh PA, **1998**.

14 Schlegel, H. B. *J. Comput. Chem.* **1982**, *3*, 214.

15 Petersson, G. A.; Al-Laham, M. A. *J. Chem. Phys.* **1991**, *94*, 6081.

16 Clark, T.; Chandrasekhar, J.; Spitznagel, G. W.; Schleyer, P. V. R. *J. Comput. Chem.* **1983**, *4*, 294.

17 Frisch, M. J.; Pople, J. A.; Binkley, J. S. *J. Chem. Phys.* **1984**, *80*, 3265.

18 Gonzalez, C.; Schlegel, H. B. *J. Phys. Chem.* **1990**, *94*, 5523.

19 Dewar, M. J. S.; Dougherty, R. C. *The PMO Theory of Organic Chemistry*, Plenum Press, New York, **1975**.

(E0204233 CHENG, B.)